

<https://doi.org/10.1038/s42003-024-06836-9>

A shared spatial topography links the functional connectome correlates of cocaine use disorder and dopamine D_{2/3} receptor densities



Jocelyn A. Ricard¹ , Loïc Labache², Ashlea Segal^{3,4}, Elvisha Dhamala⁵, Carrisa V. Cocuzza², Grant Jones⁶, Sarah W. Yip⁷, Sidhant Chopra^{2,8,9,10} & Avram J. Holmes^{2,10}

The biological mechanisms that contribute to cocaine and other substance use disorders involve an array of cortical and subcortical systems. Prior work on the development and maintenance of substance use has largely focused on cortico-striatal circuits, with relatively less attention on alterations within and across large-scale functional brain networks, and associated aspects of the dopamine system. Here, we characterize patterns of functional connectivity in cocaine use disorder and their spatial association with neurotransmitter receptor densities and transporter bindings assessed through PET. Profiles of functional connectivity in cocaine use disorder reliably linked with spatial densities of dopamine D_{2/3} receptors across independent datasets. These findings demonstrate that the topography of dopamine receptor densities may underlie patterns of functional connectivity in cocaine use disorder, as assessed through fMRI.

The study and treatment of substance use disorders represents a complex, multifaceted challenge with far-reaching implications for individuals, their families, and our broader society. In particular, increasing prevalence of cocaine use disorder substantially contributes to the rising overdose deaths in the United States¹. A fundamental question facing the field of addiction neuroscience concerns the extent to which substance use behaviors emerge through local patterns of activity or are instantiated across the broader large-scale networks of the human brain. While prior foundational work has established cortico-striatal-thalamic circuit disruption as a fundamental feature of substance use disorders², consistent with systems-level models of substance use disorders³, striatal circuitry is deeply embedded within spatially distributed and functionally linked systems that span the cortical sheet. Whether alterations in functioning are isolated to specific brain circuits or diffusely distributed throughout large-scale networks remains largely unexplored.

Cocaine preferentially targets the dopamine system, and both tonic and phasic dopamine neurotransmission have been shown to play a critical role

in the onset and maintenance of substance use pathology⁴. Here, for instance, prior work suggests that the dopaminergic system compensates by reducing the number of D_{2/3} receptors with chronic cocaine use^{5–7}. Further, reduced activity within the large-scale networks supporting attention and inhibitory control points to an imbalance between the core dopaminergic circuits that underlie subjective valuation and conditioned responding and those that support “higher-level” executive functioning. Moreover, the neuromodulatory impact of cocaine is not specific to the dopamine system, while primarily blocking the dopamine transporter and inhibiting its reuptake from the synaptic cleft, cocaine also modulates serotonin and norepinephrine transporters⁸. However, the extent to which the functional network correlates of cocaine use disorder may be coupled to the spatial distribution of dopaminergic processes, relative to other neurotransmitters, remains to be established.

Here, we investigate the relationship between cocaine use disorder, patterns of whole-brain functional connectivity, and neurotransmitter receptor densities. First, we used the network-based statistic⁹ to derive

¹Stanford Neurosciences Interdepartmental Program, Stanford University School of Medicine, Stanford, CA, USA. ²Department of Psychiatry, Brain Health Institute, Rutgers University, NJ, USA. ³Department of Neuroscience, Yale University, New Haven, CT, USA. ⁴Wu Tsai Institute, Yale University, New Haven, CT, USA. ⁵Feinstein Institutes for Medical Research, Northwell Health, Manhasset, New York, USA. ⁶Department of Psychology, Harvard University, Cambridge, MA, USA. ⁷Department of Psychiatry, Yale University School of Medicine, New Haven, CT, USA. ⁸Orygen, Melbourne, VIC, Australia. ⁹Centre for Youth Mental Health, The University of Melbourne, Melbourne, VIC, Australia. ¹⁰These authors contributed equally: Sidhant Chopra, Avram J. Holmes. ✉e-mail: ricard@stanford.edu; sc2773@rwjms.rutgers.edu; avram.holmes@rutgers.edu

whole-brain functional connectivity differences between individuals with cocaine use disorder and healthy comparison participants. We then examine the association between the identified functional network topographies and the spatial distribution of receptor densities, inferred from positron emission tomography (PET). In doing so, we demonstrate preferential correspondence between regional connectivity alterations related to cocaine use disorder and the normative topography of dopamine $D_{2/3}$ receptor densities across three independent PET datasets. These data establish that in cocaine use disorder, extensive and brain-wide alterations in connectivity exist and are closely and reliably coupled with dopamine $D_{2/3}$ receptor densities.

Results

Wide-spread connectivity alterations in cocaine use disorder

The Network Based Statistic (NBS) analyses revealed a wide-spread pattern of both hyperconnectivity and hypoconnectivity associated with cocaine use disorder, encompassing 8.8% of the total edges (8185 edges; $p_{FWE} = 0.025$) linking 432 brain regions (Fig. 1). The majority of significant edges (58.94%;

4824 total edges) demonstrated hyperconnectivity in individuals with cocaine use disorder. Here, the highest proportion of hyperconnected edges preferentially implicated the default network (Fig. 1C–E (lower triangle)). After accounting for network size (see Methods) connections within striatum and thalamic regions, and between striatum and control networks were preferentially implicated in participants with cocaine use disorder (Fig. 1D, E (lower triangle)). At a regional level, the right temporo-parietal junction, right temporal pole, left superior temporal gyrus, medial prefrontal cortex, and anterior caudate nucleus were among the areas most strongly implicated in the network of lower functional connectivity.

When considering patterns of lower connectivity in the cocaine use disorder group, hypoconnected edges accounted for 41.06% of the total significant edges (3361 total edges). The total number of hypoconnected edges demonstrated preferential within-network connectivity of the default network, as well as between-network connectivity of striatum and ventral attention networks (Fig. 1B, C (upper triangle)). When normalizing for the total size of a given network, between-network hypoconnectivity of the striatum-somatomotor networks preferentially emerged (Fig. 1E (upper

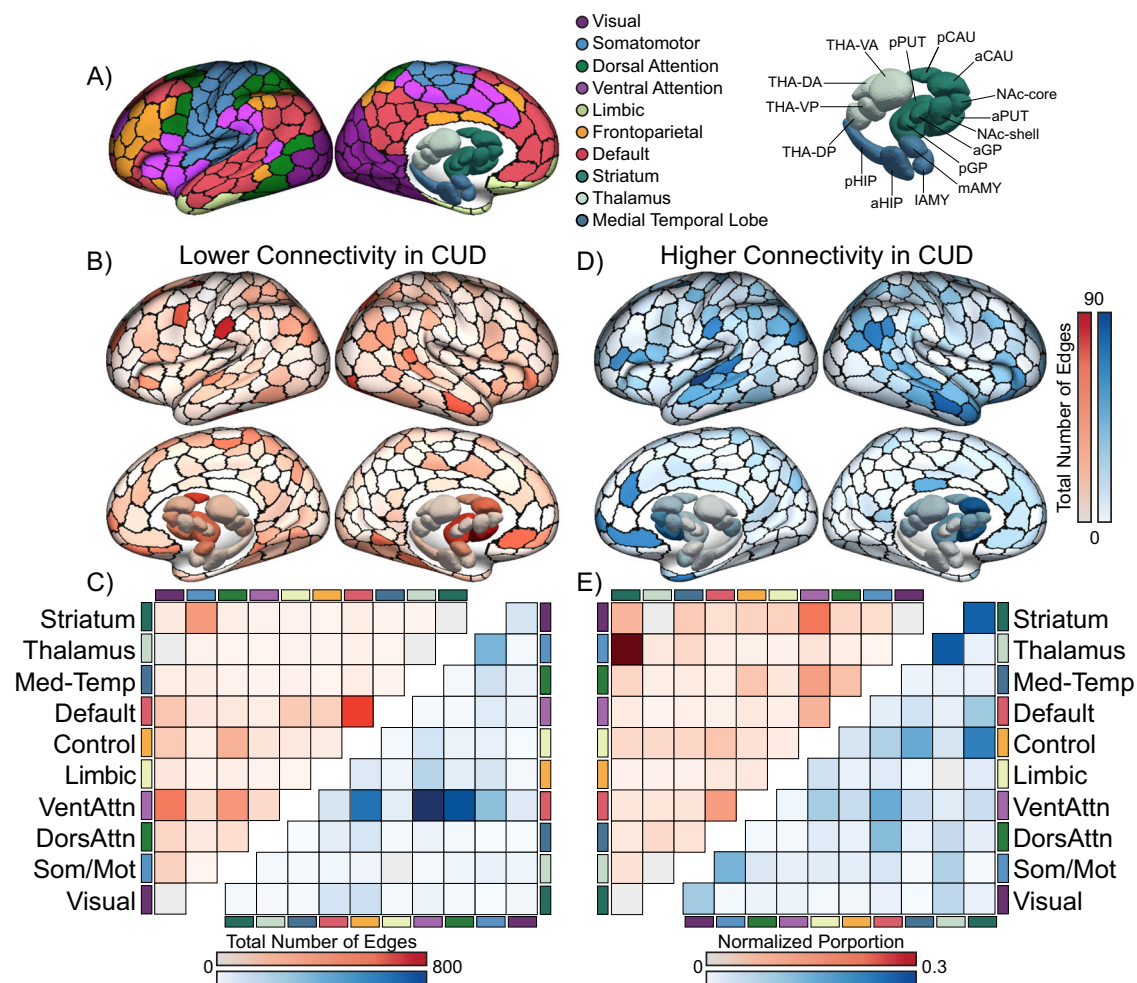


Fig. 1 | Whole brain atypical functional connectivity in cocaine use disorder. A widespread network of affected connections exists between individuals with cocaine use disorder and healthy matched comparisons, extending across the functional connectome. A Schaefer 7-network and Tian subcortex parcellations (Scale II) from left to right: a indicates anterior; AMY, amygdala; CAU, caudate nucleus; d, dorsal; DA, dorsoanterior; Default, default network; DorsAttn, dorsal attention network; DP, dorsoposterior; FPN, frontoparietal network; GP, globus pallidus; HIP, hippocampus; l, lateral; Lim, cortical limbic network; m, medial; MTL, medial-temporal lobe (amygdala and hippocampus); NAc, nucleus accumbens; p, posterior; SomMot, somatomotor network; Stri, striatum; PUT, putamen; THA, thalamus). **B** Images with a red color scale represent the number of significant positive edges (degree) where individuals with cocaine use disorder show

hypoconnectivity compared to healthy matched comparisons. Positive edges [controls > patients] = hypoconnectivity in CUD. **C** Heatmap quantified using raw total edge count for positive edges (upper triangle) and for negative edges (lower triangle). The darker red indicates lower connectivity in cocaine use disorder compared to healthy matched comparisons. The darker blue color indicates higher connectivity in cocaine use disorder. **D** Images with a blue color scale represent number of significant negative edges of NBS network where individuals with cocaine use disorder show hyperconnectivity. Negative edges [patients > controls] = hyperconnectivity in CUD. **E** Heatmap quantifies using normalized proportion of edges based upon network size for positive edges (upper triangle) and negative edges (lower triangle) within the NBS component that fall within each of the canonical networks.

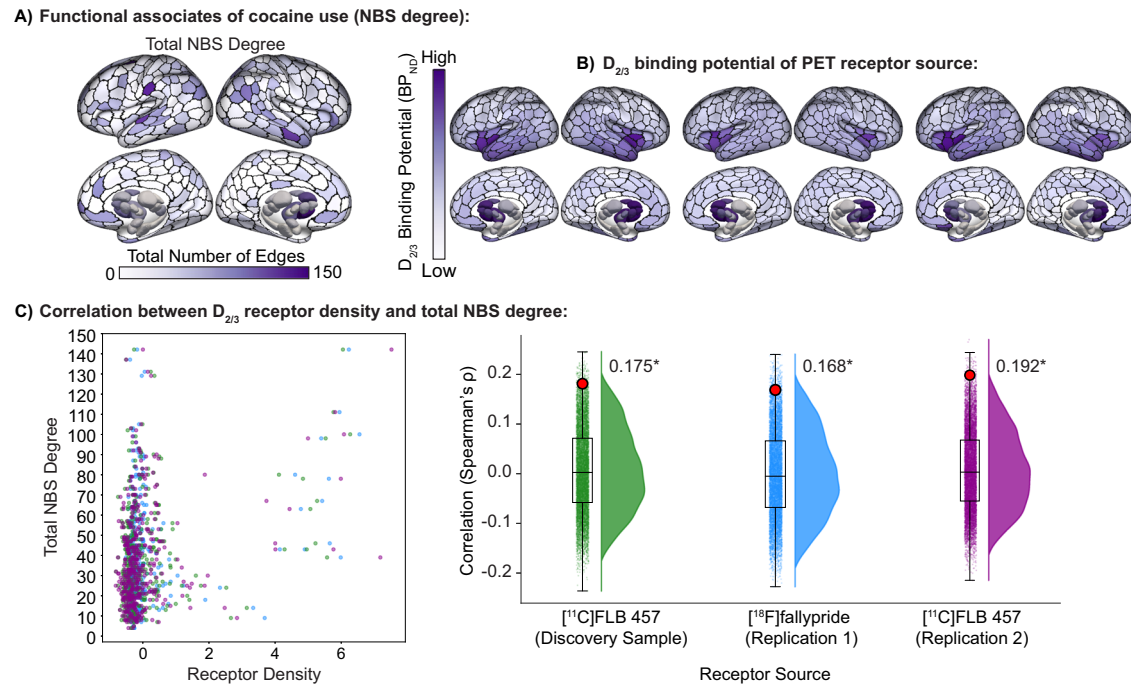


Fig. 2 | Spatial overlap between whole-brain Network Based Statistic (NBS) network and $D_{2/3}$ receptor density in cocaine use disorder. **A** Visualization of the total (positive and negative) number of significant edges at each region within the NBS component (Fig. 1B, D) where change in fMRI was significantly correlated with the spatial $D_{2/3}$ receptor density in a discovery sample (Sandiego 2015, $p_{\text{spin}} = 0.019$) and two replication samples (Jaworska 2020, $p_{\text{spin}} = 0.030$ and Smith 2017, $p_{\text{spin}} = 0.013$), respectively). **B** $D_{2/3}$ binding potential of PET samples for each receptor source, i.e., discovery sample and replication samples. Color scale normalized between -1.0 to 1.0 for cortex and subcortex separately. **C** Scatterplot shows

spearman's correlation between z-scored $D_{2/3}$ receptor density and total NBS degree. Each violin-box plot contains (from left to right) distribution of 10k spin-test null correlations between each edge of the NBS component and the spatial density of $D_{2/3}$ receptors. Red dot indicates significant spearman's correlation. * reflects statistical significance at the threshold $p_{\text{spin}} < 0.05$. Scatter and Violin plot colors reflect the associated samples. Discovery Sample: Sandiego et al.³²; Replication 1: Jaworska et al.³³; Replication 2: Smith et al.³⁴. Binding potential refers to the ratio at which a radioligand binds to a specific receptor within the brain compared to its nonspecific binding.

triangle). At a regional level, frontal operculum, parietal operculum, extrastriate cortex, and anterior putamen, were among the areas most strongly implicated in the network of lower functional connectivity in individuals with cocaine use disorder.

Shared spatial topography links cocaine use disorder and $D_{2/3}$ receptor densities

Regional patterns of altered connectivity in cocaine use disorder were significantly correlated with $D_{2/3}$ receptor densities ([^{11}C]FLB 457, $\rho = 0.175$, $p_{\text{spin}} = 0.015$). Associations with $D_{2/3}$ receptors were replicated across two additional normative PET maps ([^{18}F]fallypride, $\rho = 0.168$; $p_{\text{spin}} = 0.022$) and ([^{11}C]FLB 457, $\rho = 0.192$; $p_{\text{spin}} = 0.007$) (Fig. 2B, C), indicating robust and reliable relationships between $D_{2/3}$ receptors density and cocaine use disorder-related connectivity dysfunction (Fig. 2). To ensure that this association was not driven by large differences in tracer binding between cortical and subcortical regions, we replicated the $D_{2/3}$ receptors association after excluding subcortical regions (Supplementary Fig. 2). Associations with two serotonin results were also significant (5HT₄ [^{11}C]SB207145: $\rho = 0.143$; $p_{\text{spin}} = 0.032$, and 5HT₆ [^{11}C]GSK215083: $\rho = 0.136$; $p_{\text{spin}} = 0.020$) and reported in Supplementary Fig. 3, but did not have replication samples. No associations with other available neurotransmitter systems were detected (Supplementary Table 2). Further, associations between connectivity and $D_{2/3}$ receptors remained significant when examining hyperconnected edges only, as opposed to total numbers of implicated edges (Supplementary Table 4).

Discussion

Cocaine use disorder (CUD) emerges, in part, through the complex interactions of biological systems encompassing neurochemical cascades and associated functional interactions across both local circuits and broader

large-scale networks. Establishing how these processes contribute to the onset and maintenance of substance use disorders requires a multi-scale approach, considering measures of in vivo brain function, as assessed through fMRI, as well as neurotransmitter synthesis and transport assessed through PET imaging. In the present analyses, we find wide-spread alterations in intrinsic ("resting-state") functional connectivity in CUD and by integrating these findings with PET data, we demonstrate the presence of shared spatial patterns linking $D_{2/3}$ receptor densities with the functional connectome correlates of CUD.

While prior work has revealed disruptions in cortico-striatal-thalamic circuitry that underlie varying stages of substance use disorders², our findings highlight the presence of diffuse, brain-wide dysregulation in CUD, extending beyond neural circuit-specific hypotheses. In addition to striatal and thalamic regions, we find alterations in large-scale cortical networks, including the default, control, somatomotor, and ventral attention networks, suggesting that dysfunction extends beyond anatomically constrained cortico-striatal-thalamic circuitry.

Critically, our findings demonstrate a reliable spatial correspondence between patterns of functional connectivity in CUD and the dopaminergic system, extending across both cortical and subcortical regions. Cocaine acts by binding to the dopamine transporter, blocking the reuptake of dopamine from the synaptic cleft, as well as blocking the transporters for nor-epinephrine and serotonin⁸. While our findings also implicate parts of the serotonin system, the most replicable and robust link was found with $D_{2/3}$ receptor densities, suggesting that substance use relevant patterns of brain connectivity across large-scale brain networks are preferentially coupled to dopaminergic pathways.

Prior investigations have demonstrated distinguishable functional connectome profiles between CUD and other substance use disorders, such as opioid use disorder, suggesting that individual variability in large-scale

connectomes may serve as a valuable predictor for treatment outcomes in CUD¹⁰. While our findings demonstrate a robust pattern of functional alteration in CUD that is coupled with dopaminergic pathways, the extent to which the present findings may reflect a substance specific neurobiological profile, or a general profile related to dopaminergic drugs of misuse (for instance, opiates, alcohol, and cocaine) remains to be determined. Of note, the spatial pattern of regions with higher associated edges were correlated to those with lower associated edges (Fig. 1; $\rho = 0.317$, $p_{\text{spin}} < 0.0001$), emphasizing that rather than exhibiting a unitary relationship, such as hypo-connectivity or hyperconnectivity, implicated brain regions likely possess complex patterns of dysfunction associated with substance use behaviors.

Prior work has shown variations in D_{2/3} receptor availability among individuals with CUD^{11,12}. Additionally, in more recent research, Worhunsky et al.¹³ propose that alterations in receptor concentration could be prevalent in areas with mixed D₂ and D₃ receptors, potentially explaining the observed overlap of hyper- and hypoconnectivity patterns in our own work. Furthermore, alternate imaging techniques such as neuro-melanin MRI have demonstrated that individuals with CUD exhibited an increased neuro-melanin signal in the substantia nigra¹⁴ suggesting the degeneration or dysfunction of dopaminergic neurons. The present data, along with converging evidence of disruptions in functional connectivity observed in CUD suggesting the degeneration or dysfunction of dopaminergic neurons^{15,16}, indicate that dopaminergic alterations seen in CUD may be closely coupled with changes in large-scale functional systems.

The current study, similar to many neuroimaging datasets of individuals with substance use disorders, is limited by its cross-sectional nature and longitudinal approaches may provide further insight into whether neurobiological profiles reflect a vulnerability for illness, a direct consequence of substance use, or the byproduct of illness linked environmental impacts. Moreover, further investigations using concurrent PET and fMRI imaging in patient samples are needed to determine whether illness-related neurochemical alterations interact with brain function. In the network-level interpretations of the current study, subcortical nuclei were treated as a single network. Future work informed by the functional alignment of these nuclei to large-scale cortical systems may provide further insight into network dysfunction. Additionally, the present sample is also characterized by a large proportion of male participants. Prior work has established the importance of sex differences in the brain-behavior features that characterize substance use disorders¹⁷. Accordingly, data from more sex diverse individuals should be obtained in the future. Together, these data establish correspondence across the functional networks implicated in cocaine use disorder and the neurotransmitters that underlie its mechanism of action. This provides a foundation for future work disentangling the biological mechanisms that govern individual variances in the dopaminergic systems, functional brain organization, and substance use.

Methods

The current study used data from the SUDMEX-CUD imaging dataset¹⁸. A total of 69 individuals with cocaine use disorder (age range: 18–50, 85.51% male) and 62 demographically matched healthy comparison participants (age range: 18–48, 79.03% male) were included in the present study. Notably, these data represent a diverse and non-European-centric population in Mexico City, Mexico. Participants with cocaine use disorder had to have used for at least one year, with current average use of at least three times per week and no more than 60 continued days of abstinence during the last year. Additional participant exclusion criteria and MRI preprocessing can be found in Supplementary Sections 1–3. Participant behavioral characteristics and demographics can be found in Table 1. The reported study analyses procedures were approved by the Yale University Institutional Review Board (IRB #1507016245).

MRI acquisition and processing

Intrinsic (resting state; fMRI) functional imaging data were acquired using a 3 T Phillips Ingenia MR scanner in Mexico City, Mexico. Resting state fMRI sequences were acquired using a gradient recalled (GE) echo planar

Table 1 | Demographic characterization of study sample ($n = 131$)

Group	Cocaine Use Disorder (CUD)	Healthy Comparison (HC)	
Participants (n , % Male, % missing)	69(85.51, 1.45)	62(79.03, 3.23)	χ^2 : 0.30 $p = 0.583$
Age (mean \pm sd)	31.34 \pm 7.27	30.42 \pm 8.18	t : -0.68 $p = 0.501$
Education (% college educated, % missing)	15.94, 4.35	33.87, 6.45	χ^2 : 13.40 $p < 0.020^*$
Head Motion (mean \pm sd)	0.23 \pm 0.10	0.21 \pm 0.08	t : 1.63 $p = 0.105$

Demographic data analyses were performed on reduced sample sizes due to missing values. Specifically, age data were available for 128 participants (out of 131 total; missing 3), education data for 124 participants (missing 7), and sex data for 128 participants (missing 3; 2 in HC group, 1 in CUD group). Statistical tests used include chi-square (χ^2) for categorical variables and t-tests for continuous variables. Three participants were excluded for missing age values. Seven participants were excluded for missing education values. Three participants (2 HC, 1 CUD) missing sex values, male/female were the only available options. Head motion calculated using mean framewise displacement (mm). Asterisk (*) = significant group difference ($p < 0.05$).

imaging (EPI) sequence with the following parameters: dummies = 5, repetition time (TR)/echo time (TE) = 2000/30.001 ms, flip angle = 75°, matrix = 80 \times 80, field of view = 240 mm², voxel size = 3 \times 3 \times 3 mm, slice acquisition order = interleaved (ascending), number of slices = 36, phase encoding direction = AP.

Briefly processing involved Briefly, raw images were first put through an automated quality control procedure^{19,20} (fMRIPrep 21.0.1; RRID:SCR_016216), which is based on Nipype 1.6.1^{21,22} (RRID:SCR_002502). Data were then denoised using aComp-Cor and regressing out six-head motion parameters and mean global signal, followed by high-pass filtering (see Supplementary Section 3 for further details).

Whole-brain functional connectome correlates of cocaine use disorder

Non-parametric ANCOVA models were used to analyze brain-wide functional connectivity differences between individuals with cocaine use disorder and matched comparisons, adjusting for age, sex, and education. The Network Based Statistic (NBS) was used to perform familywise error-corrected (FWE) inference at the level of connected components of edges^{9,23}, with the primary component-forming threshold, τ , set to $p < .05$ and significance assessed at $p_{\text{FWE}} < 0.05$. Further statistical details and results for $\tau = 0.01$ and $\tau = 0.001$ are reported in the Methods and Supplementary Table 1.

Computing individual-level functional connectivity matrices

To characterize the functional profile of CUD for each individual, we used previously validated Schaefer 400 cortical²⁴ and Tian 32-Scale II subcortical²⁵ atlases (Fig. 1A) to extract regional time series by taking the average of all voxels belonging to a given region. We then calculate the pairwise Pearson correlation between each of the 432 regions, to generate 93,096 edge functional connectivity matrix. We employed the Yeo 7-network parcellation²⁶ to assign each cortical ROIs to a corresponding functional network. Subcortical regions were classified according to their broad-scale anatomy²⁵.

Functional connectivity in cocaine use disorder and receptor densities

In order to investigate the relationship between functional alterations identified in individuals with cocaine use disorder and the topographic distributions of normative neurotransmitter expression in healthy participants, we used Spearman correlation to examine spatial associations between the number of significant connections and normative receptor bindings across each of the 432-brain regions. These associations were first assessed using 18 unique spatial maps that index a specific receptor or transporter with the largest available sample size^{27,28}. Multiple maps from

independent datasets were available for some of the receptors and transporters, using either the same or unique tracer. If available, these additional maps were used to assess the stability and replicability of any statistically significant associations ($p < 0.05$). Permutation-based inference (10,000 permutations) using ‘spin-tests’ were used to assess significance, while accounting for spatial autocorrelation. Further statistical details and information regarding specific tracers are provided in the Methods and Supplementary Table 2.

Group differences in connectivity - Network Based Statistic

The Network-Based Statistic (NBS) was used to detect brain-wide differences in connectivity between individuals with CUD and healthy matched comparisons. The NBS greatly increases statistical power in brain-wide analyses by conducting statistical inference at the level of interconnected components, as opposed to single edges, which comprise groups of nodes linked together through a series of edges. Specifically, at each edge (i.e., pairwise functional connectivity estimates between two nodes), differences in functional connectivity between individuals with CUD and healthy matched comparisons were assessed using an ANCOVA, adjusting for age, sex, and education, examining the main effect of the group. The NBS procedure involves setting a primary component-forming threshold (τ), which is applied to both the observed data, and the permuted null data. The decision on where to set this threshold is arbitrary; a lower threshold can detect weaker differences over many edges, whereas a higher threshold tends to pinpoint stronger effects that might span fewer edges. We report results for $\tau < 0.05$ here, and present results for $\tau < 0.01$, and $\tau < 0.001$ in Supplementary Fig. 1 and Supplementary Table 1. For both the observed and permuted null data, we noted the size (number of edges) in the connected components above this threshold. The size of the largest component from each permutation was employed to construct a family-wise error-corrected (FWE) null distribution, and a corrected-value for each observed component was estimated as the proportion of null component sizes that was larger than the observed value at $p_{FWE} < 0.05^9$. The NBS was implemented using R-version-4.0.3, package NBR (R package version: 0.1.5)²³.

To comprehensively delineate brain-wide alterations in functional connectivity, we present the results at three different scales: (1) the level of individual connections (i.e., where edges are either under- or over-connected, or hypo- versus hyperconnectivity, respectively); (2) the level of individual brain regions, to identify specific brain areas which had a high number of significant connections (Fig. 1B, D); and (3) the level of large-scale functional brain networks, analyzed both within- and between-network. Here, we examined both as proportion of implicated edges (e.g., hypoconnectivity upper triangle, hyperconnectivity lower triangle, Fig. 1C) and as proportions normalized by the size of the network (e.g., lower triangle Fig. 1E). To determine whether the observed functional connectivity alterations showed any network-specificity, we calculated the proportion of significant edges that fell within each brain networks (e.g., Fig. 1C). Different brain networks have intrinsic differences in their size (number of regions), therefore we present both raw proportions and proportions normalized by the total number of possible network connections between each pair of networks (e.g. hyperconnectivity upper triangle, hypoconnectivity lower triangle, Fig. 1E); the former identifies preferential involvement of a given network in an absolute sense while the latter accounts for differences in network size (i.e., the tendency for larger networks to be more likely to be implicated in a given NBS network).

Normative receptor density - Neuromaps

Receptor density data were obtained from Neuromaps²⁸. Neuromaps is an open source toolbox for accessing and analyzing structural and functional brain maps, combined from open-access data to compare brain maps. Each of 34 group-level parametric PET images were parcellated into 432 regions using the same atlases as the functional MRI data, and these regional values were z-scored within each map (See Supplementary Table 2). To quantify the relationship between the various receptor distributions and CUD-related functional alterations, we first computed the degree of the detected

NBS network (number of significant edges connecting each region). We then performed Spearman’s correlation between regional degree and each receptor expression, using ‘spin tests’²⁹ for non-parametric inference that account for spatial autocorrelation (10,000 permutations²⁹). Subcortical regions were random shuffled within hemisphere at each permutation^{30,31}. Specifically, to evaluate significance between the NBS degree and receptor density maps, a corresponding set of null models was generated by permuting the NBS degree (see Methods) without replacement 10,000 times and computing the correlation with each observed receptor densities. The p -values for association with each receptor map were defined as the proportion of null models with correlation values greater than the observed value.

Reporting summary

Further information on research design is available in the Nature Portfolio Reporting Summary linked to this article.

Data availability

The neuroimaging data that support the findings for the imaging data are publicly available from SUDMEX-CONN’s OpenNeuro repository (<https://openneuro.org/datasets/ds003346/versions/1.1.2/>). Receptor density data are obtained from the neuromaps dataset (<https://neuromaps-main.readthedocs.io/en/latest/index.html>).

Code availability

The accompanying code for this project is available on GitHub (<https://github.com/ricardjocelyn/cocaine-use-disorder-receptor-density>).

Received: 3 January 2024; Accepted: 3 September 2024;

Published online: 19 September 2024

References

- Jalal, H. et al. Changing dynamics of the drug overdose epidemic in the United States from 1979 through 2016. *Science* **361**, eaau1184 (2018).
- Koob, G. F. & Volkow, N. D. Neurocircuitry of addiction. *Neuropsychopharmacology* **35**, 217–238 (2010).
- Tolomeo, S. & Yu, R. Brain network dysfunctions in addiction: a meta-analysis of resting-state functional connectivity. *Transl. Psychiatry* **12**, 41 (2022).
- Aragona, B. J. et al. Preferential Enhancement of Dopamine Transmission within the Nucleus Accumbens Shell by Cocaine Is Attributable to a Direct Increase in Phasic Dopamine Release Events. *J. Neurosci.* **28**, 8821–8831 (2008).
- Cosgrove, K. P. Imaging receptor changes in human drug abusers. *Behavioral neuroscience of drug addiction* 199–217 (2010).
- Dalley, J. W. et al. Nucleus accumbens D2/3 receptors predict trait impulsivity and cocaine reinforcement. *Science* **315**, 1267–1270 (2007).
- Martinez, D. et al. Lower level of endogenous dopamine in patients with cocaine dependence: findings from PET imaging of D 2/D 3 receptors following acute dopamine depletion. *Am. J. Psychiatry* **166**, 1170–1177 (2009).
- Nestler, E. J. The neurobiology of cocaine addiction. *Sci. Pract. Perspect.* **3**, 4 (2005).
- Zalesky, A., Fornito, A. & Bullmore, E. T. Network-based statistic: Identifying differences in brain networks. *NeuroImage* **53**, 1197–1207 (2010).
- Lichenstein, S. D., Scheinost, D., Potenza, M. N., Carroll, K. M. & Yip, S. W. Dissociable neural substrates of opioid and cocaine use identified via connectome-based modelling. *Mol. Psychiatry* **26**, 4383–4393 (2021).
- Volkow, N. et al. Stimulant-induced dopamine increases are markedly blunted in active cocaine abusers. *Mol. Psychiatry* **19**, 1037–1043 (2014).

12. Milella, M. S. et al. Cocaine cue-induced dopamine release in the human prefrontal cortex. *J. Psychiatry Neurosci.* **41**, 322–330 (2016).
13. Worhunsky, P. D. et al. Regional and source-based patterns of [11C]-(+)-PHNO binding potential reveal concurrent alterations in dopamine D2 and D3 receptor availability in cocaine-use disorder. *Neuroimage* **148**, 343–351 (2017).
14. Cassidy, C. M. et al. Neuromelanin-sensitive MRI as a noninvasive proxy measure of dopamine function in the human brain. *Proc. Natl Acad. Sci. USA* **116**, 5108–5117 (2019).
15. Hu, Y., Salmeron, B. J., Gu, H., Stein, E. A. & Yang, Y. Impaired functional connectivity within and between frontostriatal circuits and its association with compulsive drug use and trait impulsivity in cocaine addiction. *JAMA Psychiatry* **72**, 584–592 (2015).
16. Gu, H. et al. Mesocorticolimbic circuits are impaired in chronic cocaine users as demonstrated by resting-state functional connectivity. *Neuroimage* **53**, 593–601 (2010).
17. Becker, J. B., McClellan, M. L. & Reed, B. G. Sex differences, gender and addiction: Sex, Gender, and Addiction. *J. Neurosci. Res.* **95**, 136–147 (2017).
18. Angeles-Valdez, D. et al. The Mexican magnetic resonance imaging dataset of patients with cocaine use disorder: SUDMEX CONN. *Sci. Data* **9**, 1–10 (2022).
19. Esteban, O. et al. fMRIPrep: a robust preprocessing pipeline for functional MRI. *Nat. Methods* **16**, 111–116 (2019).
20. Esteban, O. et al. fMRIPrep: a robust preprocessing pipeline for functional MRI. Software. *Zenodo* <https://doi.org/10.5281/zenodo.8206595> (2018).
21. Gorgolewski, K. et al. Nipype: A Flexible, Lightweight and Extensible Neuroimaging Data Processing Framework in Python. *Front. Neuroinform.* **5**, (2011).
22. Gorgolewski, K. J. et al. Nipype. *Software* (2018).
23. Gracia-Tabuenca, Z. & Alcauter, S. *NBR: Network-Based R-Statistics for (Unbalanced) Longitudinal Samples*. <https://doi.org/10.1101/2020.11.07.373019> (2020).
24. Schaefer, A. et al. Local-global parcellation of the human cerebral cortex from intrinsic functional connectivity MRI. *Cereb. cortex* **28**, 3095–3114 (2018).
25. Tian, Y., Margulies, D. S., Breakspear, M. & Zalesky, A. Topographic organization of the human subcortex unveiled with functional connectivity gradients. *Nat. Neurosci.* **23**, 1421–1432 (2020).
26. Yeo, B. T. et al. The organization of the human cerebral cortex estimated by intrinsic functional connectivity. *J. Neurophysiol.* (2011).
27. Hansen, J. Y. et al. Mapping neurotransmitter systems to the structural and functional organization of the human neocortex. *Nat. Neurosci.* **25**, 1569–1581 (2022).
28. Markello, R. D. et al. neuromaps: structural and functional interpretation of brain maps. *Nat. Methods* **19**, 1472–1479 (2022).
29. Váša, F. et al. Adolescent Tuning of Association Cortex in Human Structural Brain Networks. *Cereb. Cortex* **28**, 281–294 (2018).
30. Alexander-Bloch, A. F. et al. On testing for spatial correspondence between maps of human brain structure and function. *Neuroimage* **178**, 540–551 (2018).
31. Markello, R. D. & Misisic, B. Comparing spatial null models for brain maps. *Neuroimage* **236**, 118052 (2021).
32. Sandiego, C. M. et al. Reference Region Modeling Approaches for Amphetamine Challenge Studies with [¹¹C]FLB 457 and PET. *J. Cereb. Blood Flow. Metab.* **35**, 623–629 (2015).
33. Jaworska, N. et al. Extra-striatal D2/3 receptor availability in youth at risk for addiction. *Neuropsychopharmacology* **45**, 1498–1505 (2020).
34. Smith, C. T. et al. The impact of common dopamine D2 receptor gene polymorphisms on D2/3 receptor availability: C957T as a key determinant in putamen and ventral striatum. *Transl. Psychiatry* **7**, e1091–e1091 (2017).

Acknowledgements

This work was supported by: Stanford University Knight-Hennessy Scholars Program (J.A.R.); National Academies of Sciences, Engineering, and Medicine's Ford Foundation Predoctoral Fellowship (J.A.R.); R01MH120080 (A.J.H.); R01MH123245 (A.J.H.); the Northwell Health Advancing Women in Science and Medicine Career Development Award (E.D.) and the Feinstein Institutes for Medical Research Emerging Scientist Award (E.D.); Australian American Association Graduate Fellowship (S.C.).

Competing interests

The authors declare no competing interests.

Additional information

Supplementary information The online version contains supplementary material available at <https://doi.org/10.1038/s42003-024-06836-9>.

Correspondence and requests for materials should be addressed to Jocelyn A. Ricard, Sidhant Chopra or Avram J. Holmes.

Peer review information *Communications Biology* thanks Marcela Ovando-Tellez, and the other, anonymous, reviewers for their contribution to the peer review of this work. Primary Handling Editors: Michel Thiebaut de Schotten and Benjamin Bessieres.

Reprints and permissions information is available at <http://www.nature.com/reprints>

Publisher's note Springer Nature remains neutral with regard to jurisdictional claims in published maps and institutional affiliations.

Open Access This article is licensed under a Creative Commons Attribution-NonCommercial-NoDerivatives 4.0 International License, which permits any non-commercial use, sharing, distribution and reproduction in any medium or format, as long as you give appropriate credit to the original author(s) and the source, provide a link to the Creative Commons licence, and indicate if you modified the licensed material. You do not have permission under this licence to share adapted material derived from this article or parts of it. The images or other third party material in this article are included in the article's Creative Commons licence, unless indicated otherwise in a credit line to the material. If material is not included in the article's Creative Commons licence and your intended use is not permitted by statutory regulation or exceeds the permitted use, you will need to obtain permission directly from the copyright holder. To view a copy of this licence, visit <http://creativecommons.org/licenses/by-nc-nd/4.0/>.

© The Author(s) 2024, corrected publication 2025